2019 SECED Conference
Earthquake risk and engineering towards a resilient world
9-10 September 2019, Greenwich, London

ON THE USE OF OPEN-SOURCE LOW-COST VIBRATION SENSING TECHNOLOGIES FOR SEISMIC ASSESSMENT IN URBAN AREAS

Timothy LEE-LEWIS[1], Christian MÁLAGA-CHUQUITAYPE[2], Nikos NANOS[3]

Abstract:

Despite their apparent limitations, Micro Electro Mechanical Systems (MEMS) printed Integrated Circuits (IC) present an exceptional cost proposition for vibration monitoring in support of seismic risk assessment in cases where their operational characteristics warrant their use. MEMS are gaining significant traction in recent year and there is a tendency amongst researchers to treat them as a mature solution to suit an increasing array of instrumentation needs irrespective of their location. This has led to the proliferation of calibration and instrumentation studies without consideration of the setting and surrounding environment. In this context, one frequently forgotten factor during the deployment and operation of MEMS based sensing units is their inherent susceptibility to Electromagnetic Interference (EMI). In this paper we discuss the use of open-source low-cost vibration sensors for earthquake engineering applications with particular attention to EMI. To this end, we convey the results of a series of tests that quantify the effect of EMI in the ability of MEMS acceleration measuring sensors in uncontrolled environments representative of urban settings. This paper focuses on 4 case studies with an array of 5 different input ground motions and different types of MEMS accelerometers. The sensor positions from known EMI sources is systematically varied and the results are benchmarked against the input signal and an industry standard IEPE Piezoelectric accelerometer. We show that there is a clear correlation between the proximity to the EMI source and the degradation of the signal to noise ratio leading to skewed acceleration measurements with up to 37% variation. This highlights the importance of awareness of the specific EMI conditions surrounding their actual deployment at a given site and calls for scepticism on studies using MEMS where EMI are not properly identified or characterized.

Introduction

The evaluation and development of structural monitoring equipment utilising components off the shelf (COTS) that incorporate novel and economical sensors has received much interest in recent years (e.g. D'Allesandro *et al.*, 2014, Yien *et al.*, 2016). Industries and organisations routinely employ various kinds of sensors as single entities or in combinations to improve their intelligence or data collection (Alavi *et al.*, 2018). It is therefore unsurprising that data collection has progressed into the continuous monitoring of structural systems (Farrar and Worden, 2007). Non-intrusive techniques called Non-Destructive Damage Evaluation (NDE) and Non-Destructive Testing (NDT) (Das and Saha, 2018) have seen breakthroughs from integration with modern technologies (Chiu and Galea, 2012) and the demand for SHM instrumentation that meet the requirements of low-cost, negligible invasive effects and analogous to that of their macro-scale equivalents (Balageas *et al.*, 2006) has increased.

The performance evaluation and calibration of various low-cost MEMS accelerometers has been the subject of a large number of studies (i.e. Evans *et al.,* 2014, Bedon *et al.,* 2018). It was during our experimental work using COTS prototypes, that Electromagnetic Interference (EMI). Related anomalies became apparent. This paper documents such anomalies and summarizes the outputs of a systematic study conducted towards their quantification. We found that these anomalies are not restricted to the inherent limitations of the MEMS devices but relate to the environments in which they are deployed. This has important implications for MEMS-based networks in urban

[1] PhD Researcher, University of Portsmouth, Portsmouth, United Kingdom, timothy.lee-lewis@port.ac.uk
[2], Senior Lecturer, Department of Civil and Environmental Engineering, Imperial College London, UK
[3], Senior Lecturer, School of Civil Engineering and Surveying University of Portsmouth, Portsmouth, UK

areas, as opposed to cases where accelerometers are assembled and tested within controlled environments purposely designed for electronic manufacture and calibration. This phenomenon of recorded interference should be a dominant factor to evaluate the vulnerability of these self-assembled devices prior to any future deployment.

EMI interference is widely recognised (Williamson, 1993) as having negative effects of intentional and unintentional transmissions and affect delicate electronic devices with respect to conducted or radiated interference and disturbance of the incoming mains supply of equipment. In response to these problems, the Comité International Sspécial des Perturbations Radioélectriques (CISPR) was founded in 1934. CISPR subsequently produced technical publications comprising of measurement and test techniques. This also extended to recommended limits upon emission and immunity of devices. Although these recommendations are applicable to today's emerging low-cost sensing technology, much equipment that is still being used from previous compliance benchmarks does not consider the increased vulnerability from higher switching speeds and lower voltages of today's devices. This highlights the importance of awareness of the specific EMI conditions surrounding the testing and deployment of open-source low-cos MEMS acceleration sensing devices and calls for scepticism on studies using MEMS where EMI are not properly identified or characterized.

COST Micro Electro Mechanical Systems Technology

Micro Electro Mechanical Systems (MEMS) technology

Micro Electro Mechanical Systems (MEMS) technology for SHM present advantages but also challenges to meet demanding goals for cost, performance, size, weight and power consumption. It is acknowledged that for effective SHM to be viable, vibrations ranging from strong motion to ambient vibration need to be perceived on large-scale structures having natural frequencies in the range of 10^{-1} to 10^{1} Hz (Chopra, 2012). In this context, MEMS present a feasible low-cost alternative (Sabato *et al.*, 2017, Cigada *et al*., 2007), as opposed to costly, high end products like Integrated Electronic Piezo Electric (IEPE) sensors. Other studies employing MEMS for vibration data collection (Jung *et al.*, 2014, Patil *et al.*, 2015) have evidenced a close agreement with data obtained from commercial available devices. Further research efforts on full scale bridges of Golden Gate (Pakzad, 2010) and Pietratagliata (Bedon *et al.*, 2018) utilising MEMS have also indicated close agreement with numerical modelling and commercially available devices.

However, MEMS devices are not without flaws. Predominantly bias drift (Gulmammadov, 2009) which is a combination of time, temperature and acceleration dependent behaviours that introduce errors has been identified as the most important. Technological advances (Chen and Huang, 2018, Isobe *et al.,* 2018, Kavitha *et al.*, 2016) have been sought to address previous problems associated with power consumption, poor noise, improved response at low frequencies due to small mass of the sensing component and noise floor that is flat to acceleration (issues at frequency < 1Hz). These previous studies have reported reduction of noise reaching 6.673 μ g/$\sqrt{}$Hz, 15ng/$\sqrt{}$Hz and 1.13 μ g/$\sqrt{}$Hz respectively, thus improving performance ideal for the purpose of SHM. However, the improvements are associated with other vulnerabilities as analog devices that sense signals in the order of a few millivolts are particularly sensitive to electromagnetic interference (Kune *et al.*, 2013) that traditional shielding techniques improve but do not eliminate. Acoustically harsh environments (Dean *et al.*, 2011) also have an adverse effect on MEMS gyroscopes when the acoustic energy frequencies components are close to the resonating frequency of the proof mass of the sensing components and there are significant resulting differences in acoustically sensitive bandwidth between otherwise identical devices because of microfabrication tolerances. Thus, current assumptions of data integrity from these devices should be brought into question. Trippel *et al.* (2017) reported, from testing of 20 accelerometers, that up to 75% of these devices are vulnerable to acoustic interference.

Micro Controller Units (MCU)

The computational core or MCU enables active data processing of attached sensors and can be tailored to specific monitoring activities. Some of these devices like Arduino©, Rapsberry Pi© and PIC© have grown in maturity alongside contemporary developments of processors with respect to speed, power and size. They have become popular as a means to receive and condition data for smart analysis as demonstrated for mechanical vibrational analysis (Varanis *et al.*, 2017), thermal compensation of MEMS sensors of tilt measurements (Ruzza *et al.*, 2018) and the urban network Geophonino-3D seismic noise recorders (Soler-Llorensa *et al.*, 2018). Appreciation and

willingness to employ these devices is also beginning to gain acceptance by other research groups involving the deterioration monitoring of building elevators (Olalere and Dewa, 2018), indoor environmental quality (Karami *et al.*, 2018), road traffic and air pollution (Zaldei *et al.*, 2017), volcanic activity monitoring (Altamirano-Santillán *et al.*, 2017). Nevertheless, problems associated with wire impedance, triboelectric noise and signal quality from attached sensors introduced data errors in these earlier systems (Sabato *et al.,* 2017). For this reason, Hsu *et al.* (1998) proposed that Wireless Sensor Networks (WSN) may present opportunities for acoustic, vibration, and magnetic field observation over large distances circumnavigating problems with wired systems. Contemporary MCU's are beginning to employ smartphone Central Processing Units (CPU), and it is interesting that seismological alarm systems have been explored with the use of cellular phones (Dashti *et al.*, 2013). Kong *et al.* (2016) suggested that earthquakes of a magnitude 5 at distances of 10 km or less can be recorded. Nevertheless, MCU's are not immune to potentially conducted and radiated noise from the MCU circuits themselves (Microchip, 2018) and should be investigated thoroughly to avoid any conflicts with other hardware within close proximity like motors, power switches, fluorescent lights, etc. The victim circuit can be disrupted easily by radiated and conducted noise. Zhu *et al.* (2019) has proposed that huddle testing after acceptable stability should be performed to ascertain noise by statistical means for calibration. Further protection against conducted noise could be implemented (STMicroelectronics, 2014) and embedded inside the software to provide preventative and auto-recovery techniques to improve hardware functionality and confidence of output from sensors.

Experimental Apparatus

Prototype sensor boards

Figure 1 shows the sensor boards employed in this study: a) Arduino MKR1000; and b) Microchip PIC40. As a comparison of size, the IEPE piezoelectric sensor DJB© equipment is seen on the far right. All sensor boards were manufactured at the University of Portsmouth and bench tested within the electronic laboratories prior to testing within the structures laboratory.

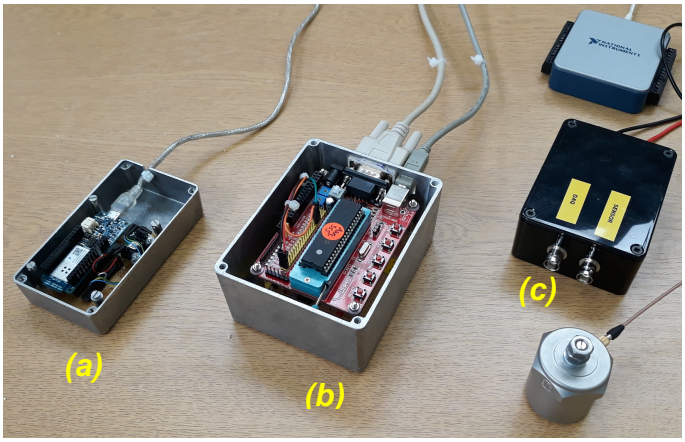

Figure 1. Sensor Boards and IEPE Piezoelectric sensor

Characteristics of microcontrollers

The characteristics of the MCU's are shown in Table 1. These values are based upon available data at the time of testing.

Characteristics of Microcontrollers					
MCU	Processor	Clock Speed MHz	ADC	ADC Bandwidth	Input Voltage
National Instruments 6003	N/A	80	OnBoard (16 Bit).	65536	5
Arduino Mega 2560	ATmega2560 (8Bit)	16	OnBoard (10 Bit).	1024	3.3-5
Arduino MKR1000	SAMD21 Cortex-M0+ (32bit)	48	OnBoard (8, 10, 12 Bit).	255,1024,4096	3.3-5
Microchip PIC40	(RISC)CPU (8Bit)	20	OnBoard (10 Bit).	1024	2-5

Table 1. Generalised basic characteristics between microcontrollers

Characteristics of accelerometers

The accelerometers are essentially all analog sensors. Digital sensors incorporate an onboard ADC circuit and were interfaced using I2C and SPI protocols, this allowed a further range of the various technologies to be evaluated. Table 2 summarizes the accelerometer specifications. Maximum sensitivity was maintained for all prototypes for testing purposes.

Characteristics of Accelerometers						
Manufacturer /Device	Analogue / Digital	Range (g)	Sensitivity	Resonance Frequency (kHz)	Noise Floor (μg√Hz)	Voltage
DJB Instruments A/1800/V	Analogue	0.5	10 V/g	4	1Hz 48μg/√Hz 10Hz 23μg/√Hz 100Hz 250ng/√Hz	15-35
NXP (MMA7361L)	Analogue	±1.5, 6	800 mV/g @ ±1.5g 206 mV/g @ ± 6g	6	350	3.3,5
InvenSense (MPU-6050)	Digital I2C (14 Bit)	±2, 4, 8,16	@ ± 2g 16,384 LSB/g @ ± 4g 8,192 LSB/g @ ± 8g 4,096 LSB/g @ ± 16g 2,048 LSB/g	400	400	2.375-3.46, VLOGIC=1.8 ±5%
ANALOG DEVICES (ADXL355)	Digital SPI/I2C (20 Bit)	± 2.048, 4.096, 8.192	@ ± 2g 256,000 LSB/g @ ± 4g 128,000 LSB/g @ ± 8g 64,000 LSB/g	1.5	25	2.25-3.6, VLOGIC=1.8 ±10%

Table 2. Generalised basic characteristics between accelerometers

Methodology

The objective of the testing campaign was to compare the data obtained for correlations between the industrial standard accelerometer device/software versus self-assembled COTS sensor boards to measure any anomalies from interference emanating from the EMI source. The shaking table consists of single degree of freedom (SDOF) heavy duty compact ball screw transmission with a stroke of 570mm with a bespoke carriage to support a table size of 1m x 0.5m in size. This is in turn is driven by a Baldor© 2.18kW, 300V 3-phase motor with a maximum speed of 2000 RPM. This equipment is typically employed within the manufacturing industry for autonomous production lines providing necessary accuracy required for continuous processing and in our case is the source of EMI. The mechanical component is controlled by the Motiflex e100 servo drive/motion controller manufactured by ABB© with Mint lite software linked via a positioning encoder on the transmission body to ensure accuracy of carriage movement with displacement. Only key findings of the campaign are reported herein with focus on the earthquakes described in Table 3.

Input Earthquakes Data Used for Intensity/Time Variation			
Place	**Date**	**Magnitude**	**Duration (s)**
Parkfield, California	June 27th 1966	5.6	44.02
Honshu, Japan	April 5th 1966	5.4	9.98
Monte Negro, Yugoslavia	April 15th 1979	7	40.38
El Suchil, Mexico	September 19th 1984	8.1	120
San Fernando, California	February 9th 1971	6.4	41.94

Table 3. Earthquake input data

Hardware testing

Preliminary hardware tests of the prototypes were undertaken within the Structures Laboratory of the University of Portsmouth. The shaking table displacement was measured against input data using double integration to verify displacement fit for purpose. Cross correlations of dataset response were performed with the A/1800/V IEPE accelerometer as a reference sensor. The IEPE sensor is considered reasonably impervious to interference but was initially checked against proposed earthquake inputs and frequency tests were conducted for inaccuracies of the sensor and shaking table hardware via Power Spectrum Density (PSD) at several frequencies. To this purpose, the shaking table was activated at the set frequencies for 1 minute with a 30 second recording window to avoid transient frequencies on start-up. To assist in the validity of the cross correlation of data obtained, analysis was performed using equation (1) Pearson Product Moment Correlation Coefficient (PPMCC) and equation (2) Root Mean Square (RMS). This allowed a

simple measure of the linearity and magnitude correlation between hardware and reference sensor as well as the sensor board prototypes.

$$PPMCC_{x,y} = \frac{\sum_i (x_i - \bar{x})(y_i - \bar{y})}{\sqrt{\sum_i (x_i - \bar{x})^2 \sqrt{(y_i - \bar{y})^2}}} \quad (1)$$

$$rms_{x,y} = \sqrt{\frac{\frac{1}{n}\sum_i x_i^2}{\frac{1}{n}\sum_i y_i^2}} \quad (2)$$

Table 4 summarizes the *PPMCC* and *rms* results from the IEPE sensor under dynamic earthquake conditions. It can be seen that with the lengthening of earthquake, compound errors occur where the shaking table hardware has difficulty in maintaining higher amplitude acceleration change of direction and phase (see Figure 2). The time acceleration plot is at primary and secondary wave conditions (for clarity).

Statistical Results IEPE/Shaking Table under Dynamic Earthquake Conditions			
Earthquake	**Duration (s)**	***PPMCC*** $_{x,y}$	***rms*** $_{x,y}$
Parkfield California	44	0.9741	0.9845
Honshu Japan	10	0.9824	0.9726
Monte Negro Yugoslavia	40	0.9728	0.9744
El Suchil Mexico	120	0.8648	0.8619
San Fernando California	42	0.9728	0.9720
Average=		0.9534	0.9531

Table 4. PPMCC and rms results for IEPE and Shaking Table hardware.

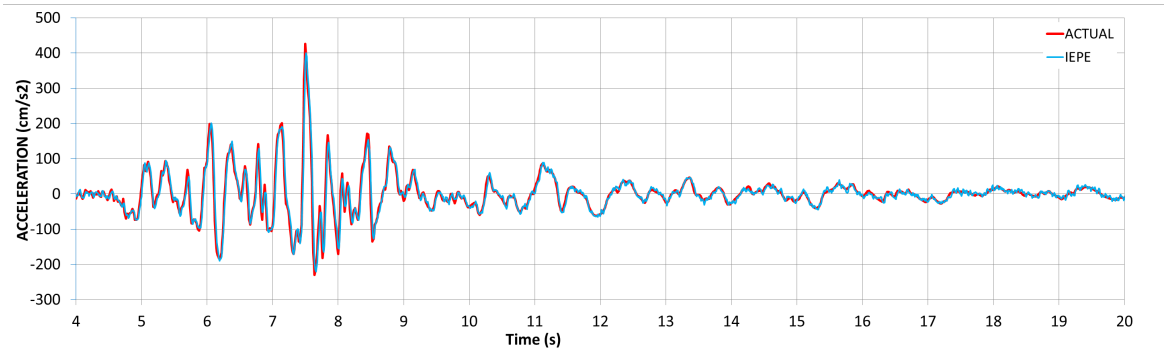

Figure 2. Input data versus IEPE data of a reduced time acceleration plot for Parkfield California Earthquake.

Statistical Results IEPE/Shaking Table under Frequency Tests		
Hz	***PPMCC*** $_{x,y}$	***rms*** $_{x,y}$
2.5	0.9671	0.9642
5	0.9604	0.9589
12.5	0.9587	0.9582
Average=	0.9621	0.9604

Table 5. PPMCC and rms results for IEPE and Shaking Table hardware.

In response to these inaccuracies, further tests were performed as a comparison of frequency response (Table 5) between the IEPE sensor and the input data of the shaking table hardware. Statistical coefficients from these tests suggest an acceptable reliability and stability for continuation of testing of the prototype sensor boards, thus PSD and acceleration time plots were elaborated and the corresponding data is shown in Table 6. This table indicates that, though less

reliable than expected, the ADXL335 accelerometer and PIC MCU provided the most favourable correlation.

X Axis Frequency Test Implementing *PPMCC*				
	2.5Hz	5Hz	12.5Hz	Average=
PIC40/ADXL355	0.668	0.675	0.673	0.672
MKR1000/ADXL355	0.588	0.610	0.592	0.597
PIC40/MPU6050	0.445	0.466	0.471	0.461
MEGA2560	0.126	0.119	0.121	0.122

Table 6. PPMCC and rms results for IEPE and Shaking Table hardware.

Noise level test

Static tests were performed with a sensor array on a framework above in close proximity to the shaking table to first ascertain the ADC baseline noise. These values were found to be less than ± 3, equivalent to a variation of ± 0.146 x 10^{-1} Volts. Tests were then performed with static framework and the table activated with the chosen earthquakes and averages were taken. Cancellation using baseline data against moving data produced a spatial map (see Figure 3) of variations in ADC values in proximity to the shaking table. Though there are manufacturing differences that cause varied sensitivity of these devices, differences in values were noted at closer proximity to the shaking table mechanism (EMI source). Higher intensity of noise was mapped with darkening red circles matching the outputs of the ADC. From this map 4 areas were chosen (highlighted with cyan borders) to measure collected datasets of the prototype for any abnormal variations.

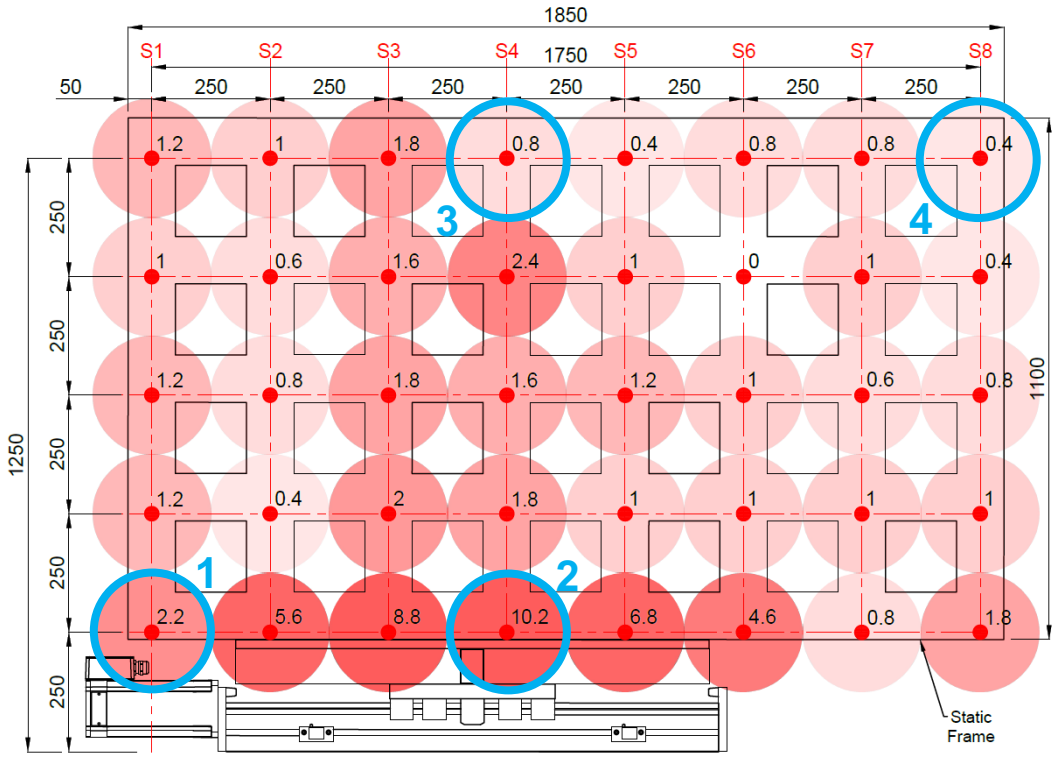

Figure 3. Static frame indicating ADC values outside baseline recording and chosen positions for prototype measurements.

Shaking table earthquake testing

The sequence of data collection was performed using different methods relevant to the accelerometer. Cross compatibility was restricted to the final datasets which were recorded as Excel CSV files. Acceleration time-plot records against actual input data of the shaking table controller were used to correlate matching acceleration and a final *PPMCC* and *rms* was performed.

Results and Discussion

As the most favorable of prototypes, the PIC40 with an ADXL was tested within dynamic conditions at set spatial positions 1 2 3 and 4 representing distances of 0.14, 0.76, 1.37 and 2.09 meters respectively, measured from the center of the drive shaking table drive motor (EMI source) to each sensor. As an example, the results for the Honshu Japan earthquake are presented in Figure 4. It is clear from this figure that a reasonable clarity of rendition is achieved by the MEMS sensor board prototype at position 3. Corrective conditioning of filtering has not been performed in the results presented in Figure 4.

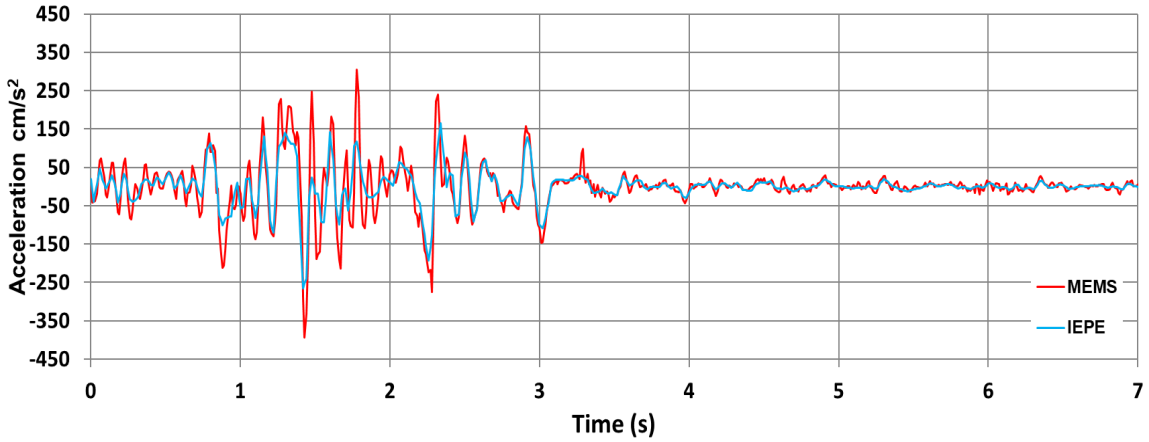

Figure 4. Honshu Japan earthquake and data at position 3.

Shown in Figure 5 is the Honshu Japan earthquake recorded at position 2. It is evident that under closer proximity to the body of the shaking table mechanism and motor, there is less clarity and the noise of the shaking table system has clouded the collected data. Finally shown in Figure 6 is the same earthquake under scrutiny but with data recorded at position 1 in direct proximity to the shaking table motor. It has become reasonable clear that the motor has a direct effect upon the data collection. It should be noted that the prototype had been encased within cast aluminium housing which represents a shielded enclosure and was earthed appropriately to the circuit.

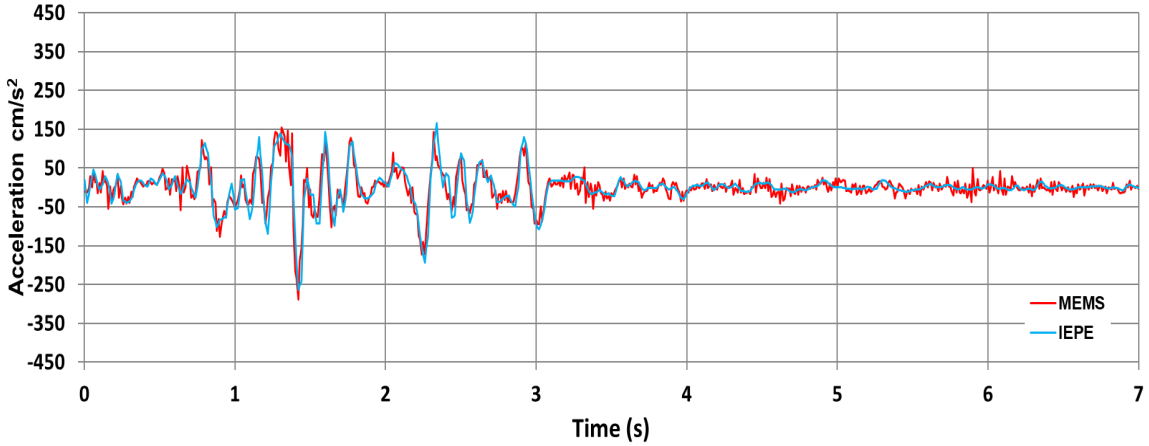

Figure 5. Honshu Japan earthquake and data at position 2.

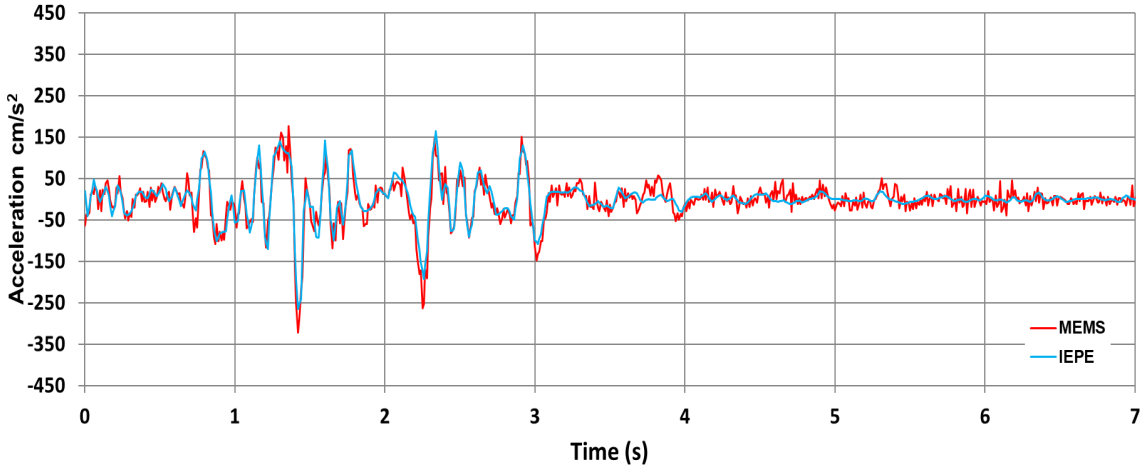

Figure 6. Honshu Japan earthquake and data at position 1.

Statistical Results of the Prototype Sensor Board and IEPE under Shaking Table Dynamic Earthquake Conditions								
Earthquake	**Duration (s)**	**Statistical test**	**PIC40/ADXL355**				**Average Prototype**	**Average IEPE**
			@ Position 1	**@ Position 2**	**@ Position 3**	**@ Position 4**		
Parkfield California	44	$PPMCC_{x,y}$	0.5044	0.5185	0.6576	0.5413	0.5554	0.9741
		$rms_{x,y}$	0.4371	0.4578	0.5899	0.4887	0.4934	0.9845
Honshu Japan	10	$PPMCC_{x,y}$	0.4867	0.5271	0.8178	0.7059	0.6344	0.9824
		$rms_{x,y}$	0.5280	0.5645	0.6539	0.5788	0.5813	0.9726
Monte Negro Yugoslavia	40	$PPMCC_{x,y}$	0.5142	0.5143	0.6958	0.6364	0.5902	0.9728
		$rms_{x,y}$	0.4961	0.5194	0.6352	0.5550	0.5514	0.9744
El Suchil Mexico	120	$PPMCC_{x,y}$	0.3168	0.4030	0.6579	0.4578	0.4589	0.8648
		$rms_{x,y}$	0.3259	0.4395	0.7529	0.4529	0.4928	0.8619
San Fernando California	42	$PPMCC_{x,y}$	0.4675	0.4870	0.5426	0.5341	0.5078	0.9728
		$rms_{x,y}$	0.4232	0.4580	0.5571	0.4607	0.4748	0.9720
		Average=	0.4500	0.4889	0.6561	0.5412	0.5340	0.9532

Table 7. PPMCC and rms results for Prototype and IEPE and Shaking Table Tests

Seen in Table 7 are the comparison results of these tests using the *PPMCC* and *rms* equations. Correlations of distance to EMI source against goodness of data indicate a lessening of error of the statistical coefficients in regard to linearity and amplitude as the measurement is taken further away. It is noted that position 4 has a far greater error attributed to proximity to other equipment within the laboratory. Throughout the other acceleration time plot graphs it has been recognized that when a sensor is nearer to the EMI source, there is a distinct worsening and added noise as depicted by the Honshu Japan acceleration time plot graphs in Figures 5 and 6. The inverse relationship between goodness of data and EMI source proximity is also evident from the data presented in Table 7 and has been systematically identified during the extended stages of experimentation not reported herein. It is further noticed that for the combined averages of *PPMCC/rms* at position 3 and position 1 a 37% percent degradation in sensitivity was recorded.

Conclusions

In this paper we have prototyped and validated self-assembled sensor boards using COTS devices. The focus of this paper has been to alert the earthquake engineering community on issues related to the appropriateness of COTS for seismic monitoring. In particular, adverse interference from EMI environments has been stressed. Based upon the observed correlations between initial testing, and industrial standard accelerometers, our prototypes have shown that development of sensor platforms via COTS can be performed quickly and lead to an embedded design within a short period. However, it is important to benchmark throughout the design process the device susceptibility to EMI noise.

Extensive frequency tests, not reported herein were conducted. Prototype testing under actual earthquakes show a good potential of MEMS for use within the laboratory environment. Rigorous testing regimes are currently under development to be employed and reasoned with in situation of deployment in mind, to not only negate the environmental influences of deployment but also the adversary disruption experienced by devices when deployed in more critical systems.

In general, digital MEMS sensor systems appear to offer a positive alternative for infrastructure sensing but improved shielding of not only the housing of the acquisition system but also enhanced shielding of the sensor within the prototype is prudent. However, the earthquake engineering community is forewarn that studies with MEMS conducted on un-controlled environments that were not purposely designed for electronic testing and manufacture should report on the steps taken to prevent EMI or their quantification, and that EMI shielding is a very important consideration for low-cost MEMS acceleration deployments in urban areas.

References

Alavi, A. H., Jiao, P., Buttlar, W. G., & Lajnef, N. (2018). Internet of Things-enabled smart cities: State-of-the-art and future trends. *Measurement: Journal of the International Measurement Confederation*, *129*(June), 589–606. https://doi.org/10.1016/j.measurement.2018.07.067

Altamirano-Santillán, E. V., Vallejo-Vallejo, G. E., & Cruz-Hurtado, J. C. (2017). Monitoreo volcánico usando plataformas Arduino y Simulink. *Revista De Investigación, Desarrollo E Innovación*, *7*(2), 317–329. https://doi.org/10.19053/20278306.v7.n2.2017.6073

Bedon, C., Bergamo, E., Izzi, M., & Noè, S. (2018). Prototyping and Validation of MEMS Accelerometers for Structural Health Monitoring—The Case Study of the Pietratagliata Cable-Stayed Bridge. *Journal of Sensor and Actuator Networks*, *7*(3), 30. https://doi.org/10.3390/jsan7030030

Bedon, C., Bergamo, E., Izzi, M., & Noè, S. (2018). Prototyping and validation of MEMS accelerometers for structural health monitoring—The case study of the Pietratagliata cable-stayed bridge. Journal of Sensor and Actuator Networks, 7(3), 30.

Balageas, D., Fritzen, C. P. and Gemes, A. "Introduction to structural health monitoring," in Structural Health Monitoring, Eds. London, U.K.: Wiley, 2006, pp. 13–15.

Chen, J-H. and Huang, C-W. (2018). 0.35 μm CMOS–MEMS low-mechanical-noise micro accelerometer. Microsyst Technol 24. pp. 299–304

Chopra, A. K. (2012). Dynamics of Structures: Theory and Applications to Earthquake Engineering. Boston, MA, USA: Prentice-Hall,

Cigada, A., Lurati, M., Redaelli, M., Vanali, M., Milano, P., & Meccanica, I. (2007). Mechanical Performance and Metrolocigal Characterization of Mems Accelerometers and Application in Modal Analysis. *Imac Xxv*.

D'Alessandro, A., Luzio, D., & D'Anna, G. (2014). Urban MEMS based seismic network for post-earthquakes rapid disaster assessment. Advances in Geosciences, 40, 1-9.

Das, S. and Saha, P. (2018). A review of some advanced sensors used for health diagnosis of civil engineering structures. Measurement, Vol 129, pp.68–90.

Dashti., S., Bray, J. D., Reilly, J., Glaser, S., & Bayen, A. (2013). iShake: The Reliability of Phones as Seismic Sensors (pp. 1–10). https://doi.org/10.1109/ISSCC.2003.1234389

Dean, R. N., Castro, S. T., Flowers, G. T., Roth, G., Ahmed, A., Hodel, A. S., … Brunsch, J. P. (2011). A characterization of the performance of a MEMS gyroscope in acoustically Harsh environments. *IEEE Transactions on Industrial Electronics*, *58*(7), 2591–2596. https://doi.org/10.1109/TIE.2010.2070772

Evans, J. R. and Allen, Richard M. and Chung, A. I. and Cochran, E. S. and Guy, Richard and Hellweg, M. and Lawrence, J. F. (2014) Performance of Several Low‐Cost Accelerometers. Seismological Research Letters, 85 (1). pp. 147-158. ISSN 0895-0695.

Farrar, C. R. and Worden, K. (2007). "An introduction to structural health monitoring," Philos. Trans. Roy. Soc. London A, Math. Phys. Sci., vol. 365, no. 1851, pp. 303–315

Gulmammadov, F. (2009). Analysis, Modeling and Compensation of Bias Drift in MEMS Inertial Sensors. RAST 2009 - Proceedings of 4th International Conference on Recent Advances Space Technologies. pp. 591-596.

Hsu, V., Kahn, J. M., & Pister, K. S. J. (1998). Wireless Communications for Smart Dust. *System*, *98*, 1–22. Retrieved from http://robotics.eecs.berkeley.edu/~pister/publications/1998/smartdust_comm_memo.pdf

Isobe, A., Kamada, Y., Oshima, T. Furubayashi, Y., Sakuma, N., Takubo, C., Watanabe, K. and Sekiguchi, T. (2018). Design of Perforated Membrane for Low-Noise Capacitive MEMS Accelerometers. *IEEE Sensors.* pp 1-4

Jung, J. W., Moon, D. J., Jung, J. W., Lee, B. L., Jung, J. W., Moon, D. J., … Lee, B. L. (n.d.). A Performance Test of a 3-axis Accelerometer and Modal Analysis A Performance Test of a 3-axis Accelerometer and Modal Analysis, (June 2014), 1–10.

Karami, M., McMorrow, G. V., & Wang, L. (2018). Continuous monitoring of indoor environmental quality using an Arduino-based data acquisition system. *Journal of Building Engineering*, *19*(January), 412–419. https://doi.org/10.1016/j.jobe.2018.05.014

Kavitha, S., Daniel, R.J. and Sumangala, K. (2016). Design and Analysis of MEMS Comb Drive Capacitive Accelerometer for SHM and Seismic Applications, Measurement 93. pp. 327-339

Kong, Q., Allen, R. M., Schreier, L., & Kwon, Y. W. (2016). Earth Sciences: MyShake: A smartphone seismic network for earthquake early warning and beyond. *Science Advances*, *2*(2), 2–9. https://doi.org/10.1126/sciadv.1501055

Kune, D. F., Backes, J., Clark, S. S., Kramer, D., Reynolds, M., Fu, K., … Xu, W. (2013). Ghost talk: Mitigating EMI signal injection attacks against analog sensors. *Proceedings - IEEE Symposium on Security and Privacy*, 145–159. https://doi.org/10.1109/SP.2013.20

Microchip. (2018). Low-EMI and Electrically Robust PIC ® Microcontrollers Designed for EMC. Retrieved from http://ww1.microchip.com/downloads/en/devicedoc/61102e.pdf

Olalere, I. O., & Dewa, M. (2018). Early Fault Detection of Elevators Using Remote Condition Monitoring Through Iot Technology. *South African Journal of Industrial Engineering*, *29*(4), 17–32. https://doi.org/10.7166/29-4-1947

Pakzad, S. N. (2010). Development and deployment of large scale wireless sensor network on a long-span bridge. *Smart Structures and Systems*, *6*(5–6), 525–543. https://doi.org/10.12989/sss.2010.6.5_6.525

Patil, R. P., Chaudhari, V. D., & Rane, K. P. (2015). ARM based 3-axis seismic data acquisition system using Accelerometer sensor and Graphical User Interface. *International Journal of Engineering Research and General Science*, *3*(2), 833–838. Retrieved from http://pnrsolution.org/Datacenter/Vol3/Issue2/118.pdf

Ruzza, G., Guerriero, L., Revellino and Guadagno, F.M. (2018). Thermal Compensation of Low-Cost MEMS Accelerometers for Tilt Measurements. Sensors. Vol 18(8). pp. 1-18.

Sabato, A., Niezrecki, C., & Fortino, G. (2017). Wireless MEMS-Based Accelerometer Sensor Boards for Structural Vibration Monitoring: A Review. *IEEE Sensors Journal*, *17*(2), 226–235. https://doi.org/10.1109/JSEN.2016.2630008

Soler-Llorensa, J-L., Galiana-Merinob, J.J., Giner-Caturlaa, J.J, Jauregui-Eslavaa, P., Rosa-Cintasa, S. and Rosa-Herranzb, J. (2018). Design and test of Geophonino-3D: A low-cost three-component seismic noise recorder for the application of the H/V method. *Sensors and Actuators A: Physical*, *269*, 342–354. https://doi.org/10.1016/j.sna.2017.11.047

STMicroelectronics. (2014). Software techniques for improving microcontrollers EMC performance. Retrieved from https://www.st.com/content/ccc/resource/technical/document/application_note/1c/6c/02/93/79/c8/4e/32/CD00004037.pdf/files/CD00004037.pdf/jcr:content/translations/en.CD00004037.pdf

Trippel, T., Weisse, O., Xu, W., Honeyman, P., & Fu, K. (2017). WALNUT: Waging Doubt on the Integrity of MEMS Accelerometers with Acoustic Injection Attacks. *Proceedings - 2nd IEEE European Symposium on Security and Privacy, EuroS and P 2017*, (April), 3–18. https://doi.org/10.1109/EuroSP.2017.42

Varanis, M., Silva, A. L., & Mereles, A. G. (2017). On mechanical vibration analysis of a multi degree of freedom system based on arduino and MEMS accelerometers. *Revista Brasileira de Ensino de Física*, *40*(1), 1–11. https://doi.org/10.1590/1806-9126-rbef-2017-0101

Williamson, T. O. M., & Engineer, M. C. O. A. Designing Microcontroller Systems for Electrically Noisy Environments (1993).

Yin, R. C., Y. M. Wu, and T. Y. Hsu (2016). Application of the low-cost MEMS-type seismometer for structural health monitoring: A pre-study, Instrumentation and Measurement Technology Conference Proceedings (I2MTC), 2016 IEEE International, doi: 10.1109/ I2MTC.2016.7520389.

Zhu, Z., Au, S. K., & Wang, X. (2019). Instrument noise calibration with arbitrary sensor orientations. *Mechanical Systems and Signal Processing*, *117*, 879–892. https://doi.org/10.1016/j.ymssp.2018.07.052